

Numerical Investigation of the Effect of Corner Radius on Flow in Buildings with a 1:2 Aspect Ratio

Ahmet Efe YILDIZ
Department of Mechanical Engineeringline
Ondokuz Mayıs University
Samsun, Türkiye

Muhammet ÖZDOĞAN
Department of Mechanical Engineeringline
Ondokuz Mayıs University
Samsun, Türkiye

Abstract - In this study, the effect of the corner radius on the flow characteristics around a prismatic building with a 1:2 aspect ratio is numerically investigated using computational fluid dynamics (CFD) methods. For this purpose, four different building models were considered: a sharp-cornered square cross-section and three rounded-corner configurations with corner radii equal to 0.1A, 0.2A, and 0.3A, where A denotes the building width. Numerical analyses were performed using ANSYS Fluent under steady, incompressible, and turbulent flow assumptions, employing the standard $k-\epsilon$ turbulence model.

The flow field was evaluated in terms of pressure distribution, velocity field, streamlines, turbulent kinetic energy, drag coefficient, and surface heat flux. The results show that the application of a corner radius significantly alters the flow separation behavior and the wake region formed behind the building. The drag coefficient, calculated as 3.27 for the square cross-section building model, decreased by approximately 28% to 2.36 for the building model with a 0.1A corner radius. Further increases in the corner radius resulted in only limited additional reductions in the drag coefficient. It was determined that the minimum pressure value decreased by approximately 68% when transitioning from the square cross-section building model to the building model with a 0.1A corner radius. Heat transfer results revealed that the heat transfer per unit volume increased by approximately 31% for a 0.1A corner radius, while for larger corner radii, the heat flux distribution became more homogeneous, with only limited additional changes. Consequently, it was concluded that the corner radius has a decisive effect on building aerodynamics and thermal performance, with 0.1A emerging as a critical threshold radius.

Keywords— *Flow around a building; CFD; corner radius; drag coefficient; turbulent flow; Heat transfer*

I. INTRODUCTION

As the negative effects of global warming continue to increase, the constant growth in the world's population is also significantly raising the demand for energy. This situation necessitates a reassessment of existing energy consumption. Improving energy efficiency and promoting the use of clean and renewable energy sources are among the key components of this process.

In this context, the investigation of wind flow around buildings represents an important research area for the design of energy-efficient structures and the integration of wind-energy-based systems into buildings. However, the inherently complex

and highly variable nature of wind flow further increases the engineering significance of this topic. While average wind speeds create static loads on structures, turbulent wind behavior induce significant dynamic effects [1].

Therefore, various design and control methods are being developed to reduce wind-induced vibrations and oscillations, especially in tall structures such as skyscrapers and engineering structures sensitive to oscillation, such as bridges. One of these methods is designing the building geometry based on aerodynamic principles. Furthermore, examining the wind flow around buildings is also of great importance in terms of evaluating the effects of architectural features on pedestrian-level wind comfort [2]. Numerous studies in the literature have investigated the flow characteristics around buildings. In most of these studies, buildings have been modeled as prismatic bodies within the flow field. Researchers [3–8] conducted various analyses to examine the influence of turbulence models used in the numerical simulation of flow around buildings and compared the numerical results with experimental data. As a result of these studies, it was reported which turbulence model was more suitable for the geometry and boundary conditions examined.

The literature also contains numerous studies investigating the effect of building geometry on the flow around buildings. These studies can be categorized under different headings based on the geometric parameters considered.

Studies examining the effect of building dimensions and dimension ratios on the flow field [9,10] investigated the effects of parameters such as the building width-to-height ratio, scale effect, and depth ratio on wind flow. Additionally, some studies [11,12] have examined the effects of roof shape and roof slope angle on the flow structure around buildings. Furthermore, studies investigating the effect of the corner geometry of prismatic buildings on the flow field are also available in the literature [14]. Studies examining the effect of the distance and position of buildings on the flow field have analyzed multiple buildings placed within the flow field [14–17]. Fertelli and Balta [14] numerically examined the effects of changes in the distance between two consecutively positioned buildings on the flow field; they noted that the highest pressure coefficient values were formed on the windward surface of the front building and that these values increased with building height. Gölbaşı et al. [15] numerically and experimentally investigated the effect of inter-building distance in groups of three buildings positioned crosswise to each other. Duran and Açikel [16] numerically

investigated the effect of the distance between buildings and wind speed on the drag coefficient for three buildings positioned one in front and two behind each other at different wind speeds. They showed that the drag coefficient was not significantly affected by changes in wind speed but increased with increasing distance between buildings. Cürebal and Özmen [17] numerically examined the effects of two buildings positioned at an angle on the flow field.

Research on the flow around buildings is not limited to these topics. Studies examining the effect of wind incidence angle on the flow around buildings also occupy an important place in the literature [18,19]. Beyond these topics, studies addressing different aspects of the flow around buildings are also present in the literature. Montazeri and Blocken [20] evaluated the effects of balconies on the flow structure and pressure distributions around buildings through average pressure coefficient distributions. Özdoğan and colleagues [21] investigated the effects of modeling the flow around a solid body in two and three dimensions on the results.

In this study, the effect of corner radius on wind flow around a building was numerically investigated. For this purpose, four different building models with a 1:2 aspect ratio and different cross-sectional geometries were considered; the analyses were performed using the ANSYS Fluent software package, which is based on computational fluid dynamics (CFD). Accordingly, the aim was to elucidate the effects of corner radius variation on the flow structure and aerodynamic behavior.

II. MATERIALS AND METHODS

The corner radius of a building has a decisive effect on flow separation behavior, vortex formation, and the resulting aerodynamic loads. In prismatic buildings with sharp corners, the flow separates prematurely due to abrupt velocity and pressure gradients in the corner regions, leading to the formation of strong vortex structures and elevated turbulence levels in the wake region. Applying a radius to the corner regions allows the flow to be directed more smoothly around the corner, delaying flow separation. In this study, the effects of the radius at the corners of the building on the flow around the building and heat loss were investigated numerically.

A. Problem Definition

In this study, the effect of corner radius on the flow around a building with a 1:2 aspect ratio was numerically investigated. For this purpose, four different building models were created: one with a square cross-section and three with rounded corners. The building was modeled as a prismatic structure with dimensions of $20\text{ m} \times 20\text{ m} \times 40\text{ m}$. To reduce the computational cost and solution time, both the building geometry and the computational domain were scaled down by a factor of $1/200$ in the numerical model. In the analyses, the building height, aspect ratio, and computational domain dimensions were kept constant, while only the corner radius was varied. In the rounded-corner models, the corner radius was set to 0.1, 0.2, and 0.3 times the building width, respectively. The isometric views and section geometries of the building models examined are given in Figure 1.

The dimensions of the computational domain were defined based on the methodology proposed by Özdoğan et al. [38]. The dimensions of the solution area were defined according to the width of the building, as shown in the schematic view of the

solution area in Figure 2. Taking the building width ($A=50\text{ mm}$) as a reference, the length of the solution region was taken as $34.8A$ (1740 mm), the width as $19.8A$ (990 mm), and the height as $10A$ (500 mm). Air is assumed to enter the computational domain through the inlet with a uniform velocity of 5 m/s and a temperature of 273 K . The turbulence intensity of the air at the inlet section is 5% , and the hydraulic diameter is taken as 0.1 m , which is the height of the building. A pressure outlet boundary condition is applied at the outlet of the computational domain. The side and top surfaces of the computational domain were defined using symmetry boundary conditions, whereas the ground and building surfaces were modeled as no-slip walls. The ground was assumed to be adiabatic, and the building surfaces were assumed to have a constant surface temperature of 283 K .

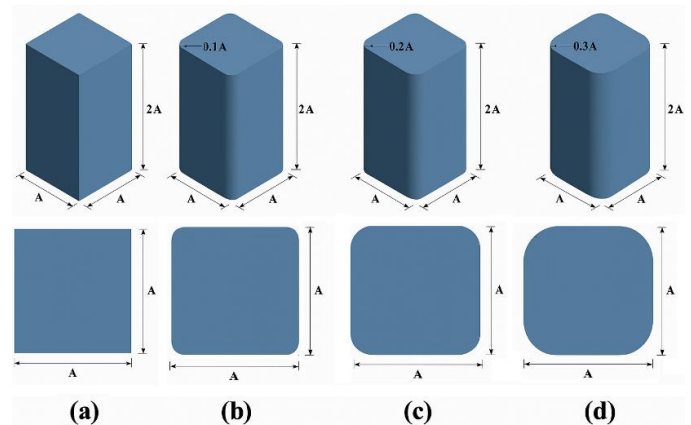


Figure 1. Building geometries with corner radius equal to 0.1 (b), 0.2 (c), and 0.3 (d) times the building width

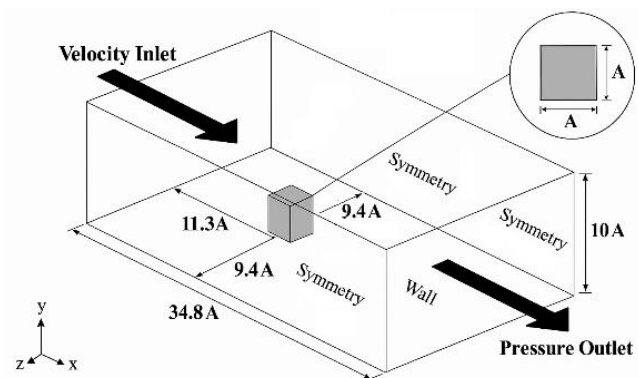


Figure 2. Schematic view of the solution domain

B. Numerical Model

The simulations were performed using ANSYS Fluent under steady-state, incompressible, and turbulent flow assumptions. When creating the model, it was assumed that the properties of air do not change with temperature and pressure. In the numerical solution, the continuity, momentum, and energy conservation equations were solved. The energy equation was included in the solution to evaluate the heat flux distributions on the building surfaces, and the heat transfer results were considered in addition to the aerodynamic results. The governing equations were discretized using a second-order upwind scheme. The SIMPLE algorithm was employed for pressure-velocity coupling. During the iterative solution

process, convergence criteria of 10^{-6} for the energy equation and 10^{-4} for the remaining equations were applied.

Continuity equation:

$$\frac{\partial U_i}{\partial x_i} = 0$$

Energy equation:

$$U_j \frac{\partial T}{\partial x_j} = \frac{\partial}{\partial x_j} \left(\alpha \frac{\partial U_i}{\partial x_j} - \overline{u_i t} \right)$$

The momentum equation:

$$U_j \frac{\partial U_i}{\partial x_j} = \frac{\partial}{\partial x_j} \left(\nu \frac{\partial U_i}{\partial x_j} - \overline{u_i u_j} \right) - \frac{1}{\rho} \frac{\partial P}{\partial x_i}$$

In these equations, the variables represent the following: U_i represents the average velocity vector, α represents the heat diffusion coefficient, P represents the average pressure, ρ represents the fluid density, and ν represents the kinematic viscosity.

The flow is assumed to be turbulent, and the standard k- ϵ turbulence model, which is commonly preferred for computational time and accuracy balance in external flow problems around buildings, is used for turbulence modeling [22]. The transport equations solved for turbulent kinetic energy (k) and turbulent kinetic energy dissipation rate (ϵ) in the standard k- ϵ turbulence model are given below:

$$\begin{aligned} \frac{\partial}{\partial t}(\rho k) + \frac{\partial}{\partial x_i}(\rho u_i k) &= \frac{\partial}{\partial x_j} \left[\left(\mu + \frac{\mu_t}{\sigma_k} \right) \frac{\partial k}{\partial x_j} \right] + G_k + G_b - \rho \epsilon - Y_M \\ &\quad + S_k \\ \frac{\partial}{\partial t}(\rho \epsilon) + \frac{\partial}{\partial x_i}(\rho u_i \epsilon) &= \frac{\partial}{\partial x_j} \left[\left(\mu + \frac{\mu_t}{\sigma_\epsilon} \right) \frac{\partial \epsilon}{\partial x_j} \right] + S_\epsilon + C_{1\epsilon} \frac{\epsilon}{k} (G_k \\ &\quad + C_{3\epsilon} G_b) - C_{2\epsilon} \rho \frac{\epsilon^2}{k} \end{aligned}$$

In these equations, k represents the turbulent kinetic energy; ϵ represents the dissipation rate of turbulent kinetic energy; $C_{1\epsilon}$, $C_{2\epsilon}$, and $C_{3\epsilon}$ represent equation constants; G_k represents the turbulent kinetic energy production due to the mean velocity gradient; G_b represents the turbulent kinetic energy production due to lift forces; σ_k , the turbulence Prandtl number for k; σ_ϵ , the turbulence Prandtl number for ϵ ; Y_M , the contribution of the total absorption rate to the separation of compressible turbulence; S_k and S_ϵ represent user-defined source terms. The coefficients used in the standard k- ϵ turbulence model are given in Table 1.

Table 1. Constants used in the standard k- ϵ turbulence model

Constant	Value
σ_k	1.0
σ_ϵ	1.0
$C_{1\epsilon}$	1.44
$C_{2\epsilon}$	1.92
C_μ	0.09

C. Mesh Structure

In the finite volume method employed by the ANSYS software package, the computational domain is discretized into a finite number of control volumes, and the governing equations are solved for each volume. Therefore, generating an appropriate mesh structure is crucial for obtaining accurate and reliable numerical results. Since the use of structured grids may lead to convergence difficulties in models with rounded corners, a tetrahedral mesh structure was adopted for discretizing the computational domain. The isometric view of the solution domain divided into cells is shown in Figure 3. During mesh generation, regions with high velocity gradients, particularly around building corners, were refined using a denser mesh. Mesh quality metrics and convergence behavior were carefully examined to ensure the reliability of the numerical solution.

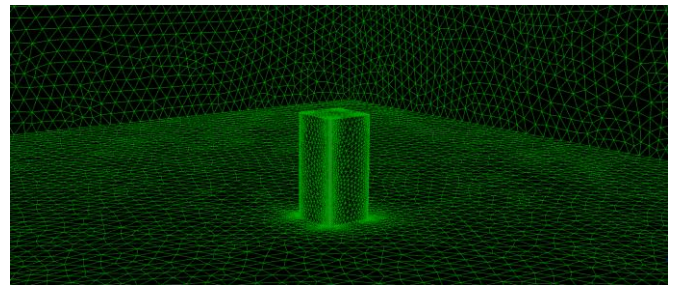


Figure 3. Mesh structure created for the building model with corner radius

In numerical simulations, the solution may vary depending on the mesh resolution. Therefore, a mesh independence study was conducted to verify that the numerical solution is independent of the mesh resolution. To verify that the numerical solution is independent of the mesh structure, six different mesh structures were created and analyzed for a building model with a corner radius equal to 0.1 times the building width. The drag coefficient obtained from the analyses and the number of cells in the mesh structures are presented in Table 2. While an approximately 3% difference was observed between the drag coefficients obtained using Grid-1 and Grid-2, the difference between Grid-4 and Grid-5 was reduced to approximately 0.04%. Based on these results, Grid-5 was selected for all subsequent simulations.

Table 2. Results of mesh independence test for

Mesh Structure	Number of Cells	Drag Coefficient (CD)
Grid-1	410174	2.222
Grid-2	430473	2.288
Grid-3	487250	2.334
Grid-4	636523	2.362
Grid-5	675320	2.361
Grid-6	785748	2.362

III. RESULTS AND DISCUSSION

In this study, the effect of the radius size created at building corners on the flow around the building has been numerically investigated. For this purpose, pressure distributions, velocity streamlines, turbulent kinetic energy (TKE), and drag coefficient (CD) values obtained at the mid-plane of the building height ($y = A$) were comparatively examined for four different building models with corner radii of 0.1A, 0.2A, and 0.3A, as well as the sharp-cornered case.

To investigate the effect of the radius of curvature at the corners of the building on the pressure distribution, contour plots of the pressure distribution formed at the mid-plane of the building height ($y=A$) are shown in Figure 4. Upon examining the figure, it is observed that the maximum pressure values occur on the front surface directly facing the wind in all building models. In the square cross-section building model, the maximum and minimum pressure values are 16.98 Pa and -24.72 Pa, respectively, whereas in the building model with a corner radius of 0.1A, the minimum pressure decreases to -41.62 Pa. This indicates that a small corner radius locally accelerates the flow, leading to increased velocity magnitudes and the formation of lower-pressure regions.

It was observed that increasing the corner radius to values of 0.2A and 0.3A resulted in minimum pressure values rising to -32.50 Pa and -28.52 Pa, respectively. These results indicate that the effect of the corner radius on the flow reaches saturation beyond a certain value, and the change in pressure distribution remains limited. The obtained pressure distributions demonstrate that the corner geometry directly affects the aerodynamic loads on the building.

Figure 5 presents the streamlines and velocity contours illustrating the effect of corner radius on the flow field. In the square cross-section building model, early flow separation occurs at the corner regions, resulting in the formation of a wide wake region downstream of the building. In building models with a corner radius applied, it was observed that the flow is directed more smoothly around the corner and flow separation is delayed.

The maximum velocity is 6.05 m/s in the square-section building model, increasing to 7.54 m/s for the building model with a corner radius of 0.1A. This increase is due to the corner radius accelerating the flow in a narrow region. Increasing the corner radius to 0.2A and 0.3A values resulted in maximum velocity values decreasing to 7.25 m/s and 7.09 m/s, respectively. This indicates that increasing the corner radius reduces local flow acceleration and results in a more uniform velocity distribution.

Figure 6 shows the turbulence kinetic energy distributions as contour plots. As can be seen from the figure, the highest maximum TKE value was obtained in the building model with a corner radius of 0.1A ($5.25 \text{ m}^2/\text{s}^2$). The maximum TKE value in the square-section building model was calculated as $4.88 \text{ m}^2/\text{s}^2$. It was determined that increasing the corner radius to 0.2A and 0.3A resulted in maximum TKE values decreasing to $4.88 \text{ m}^2/\text{s}^2$ and $4.07 \text{ m}^2/\text{s}^2$, respectively.

These results demonstrate that a small corner radius can intensify local turbulence; however, as the corner radius increases, the wake vortices weaken and the overall turbulence level decreases. In particular, it was observed that the wake region of the building model with a 0.3A corner radius had a shorter and more regular structure.

The change in the drag coefficient according to the corner radius is shown in Figure 7. The drag coefficient (CD) is calculated as 3.27 for the square cross-section building model. Increasing the corner radius to 0.1A reduces the drag coefficient to 2.36, corresponding to a reduction of approximately 28%. Increasing the corner radius to 0.2A and 0.3A resulted in more limited changes in the drag coefficient, yielding Cd values of 2.28 and 2.23, respectively.

These results show that applying a corner radius significantly reduces aerodynamic drag, but beyond a certain radius value, additional gains become limited. Accordingly, a corner radius of 0.1A can be considered a critical threshold value for aerodynamic performance.

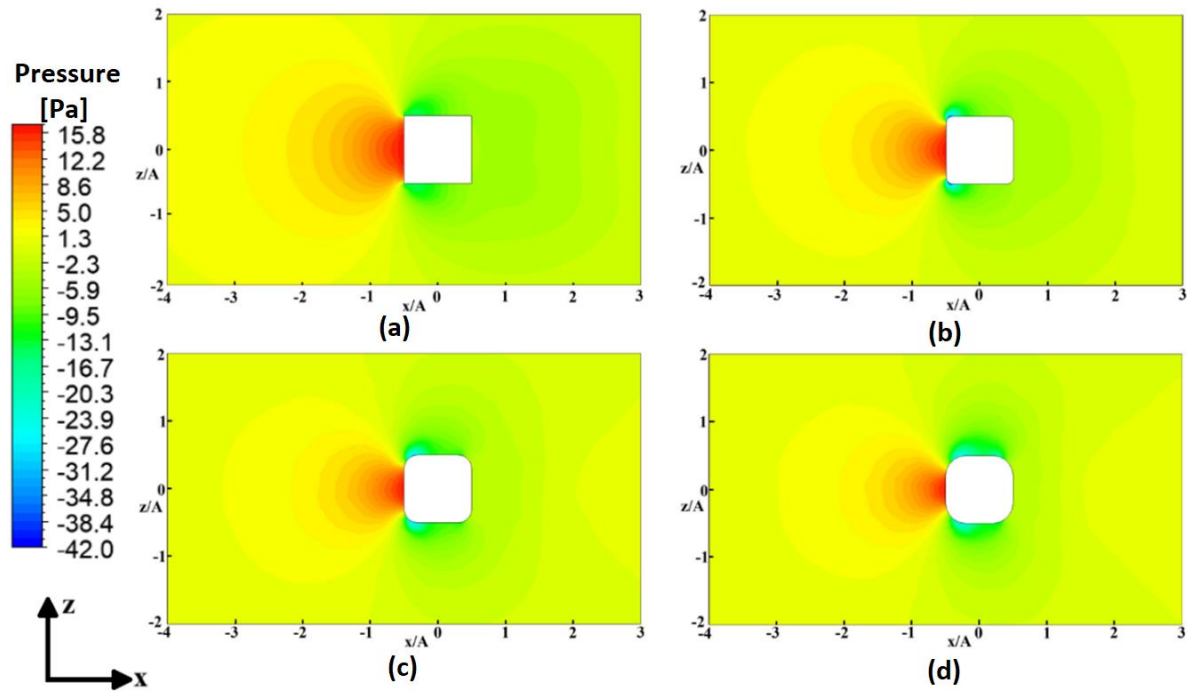


Figure 4. Pressure distribution in buildings with corner radius of square (a), 0.1A (b), 0.2A (c), and 0.3A (d)

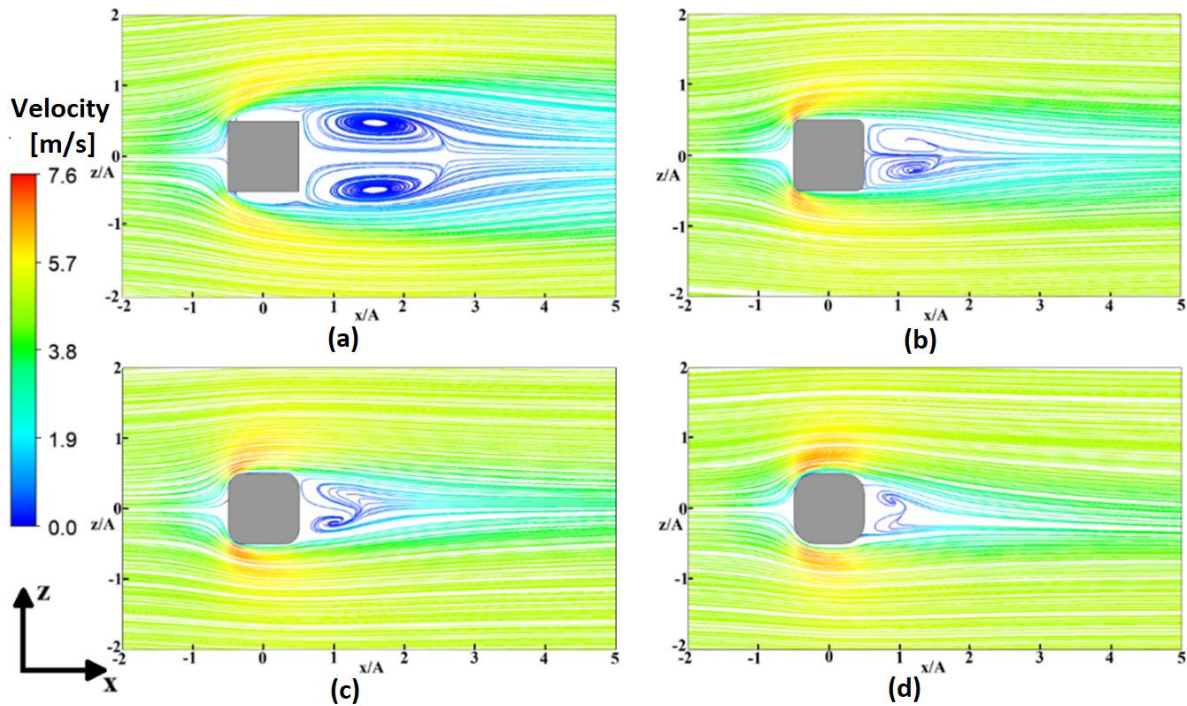


Figure 5. Flow lines and velocity distribution in buildings with corner radius of 0.1A (a), 0.2A (c), and 0.3A (d)

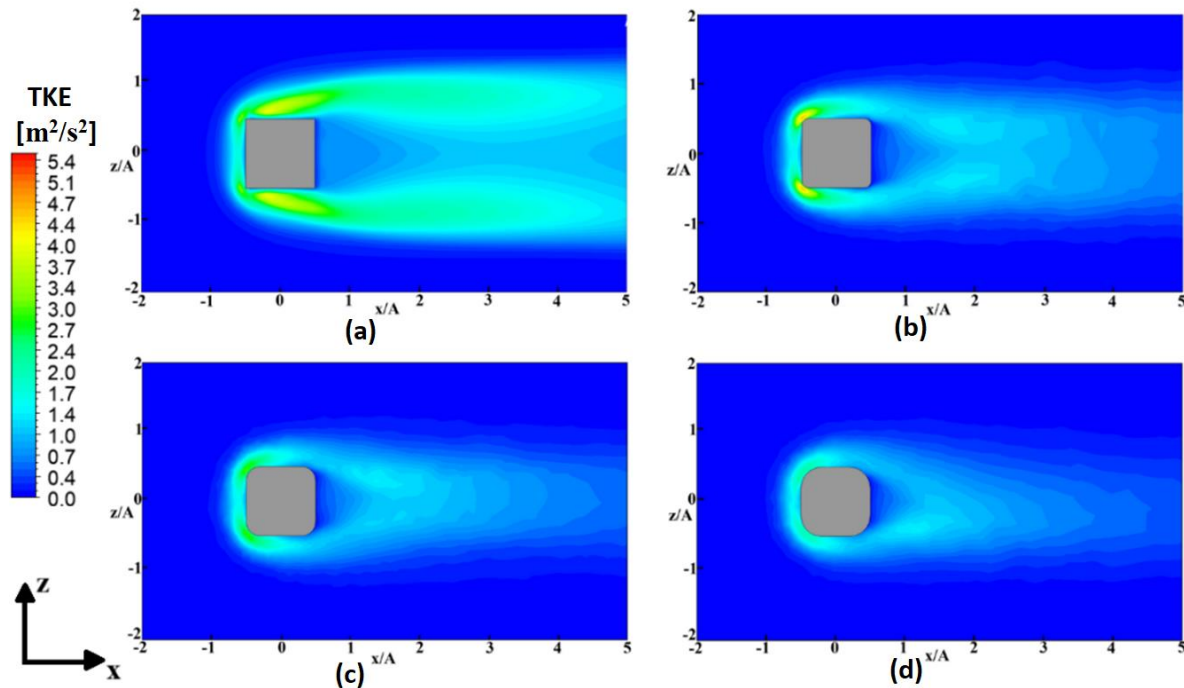


Figure 6. Distribution of turbulent kinetic energy in buildings with corner radius sections of Square (a), 0.1A (b), 0.2A (c), and 0.3A (d)

Figure 8 presents contour plots of the calculated surface heat flux distributions for building models with different corner radius. Looking at the figure, it can be seen that in the square-section building model (Figure 8-a), high heat flux values are concentrated particularly in the upper and side edge regions of the front surface facing the wind. In these regions, the sudden acceleration and early separation of air due to sharp corners increase local convective heat transfer.

With the corner radius increased to 0.1A (Figure 8-b), it was observed that the high heat flux regions spread over a wider area along the front surface and the maximum heat flux levels increased significantly. This increase can be attributed to delayed flow separation and enhanced boundary-layer development induced by corner rounding.

When the corner radius is increased to values of 0.2A and 0.3A (Figures 8-c and 8-d), the heat flux distributions become more homogeneous (); however, only limited changes occur in the maximum and average heat flux values. This indicates that the influence of corner radius on the flow structure reaches saturation beyond a certain value, and further rounding has only a marginal effect on convective heat transfer.

As a result, increasing the corner radius changes the flow characteristics around the building, affecting boundary layer development and turbulence structures; consequently, the convective heat transfer mechanism is directly affected. In particular, a corner radius of 0.1A stands out as a critical threshold value in terms of heat transfer performance.

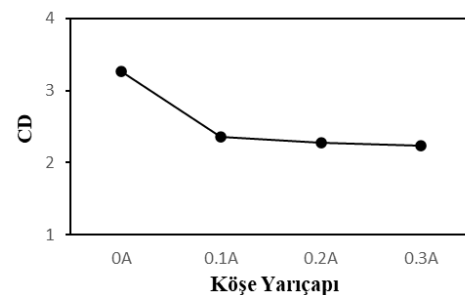


Figure 7. Change in drag coefficient according to corner radius

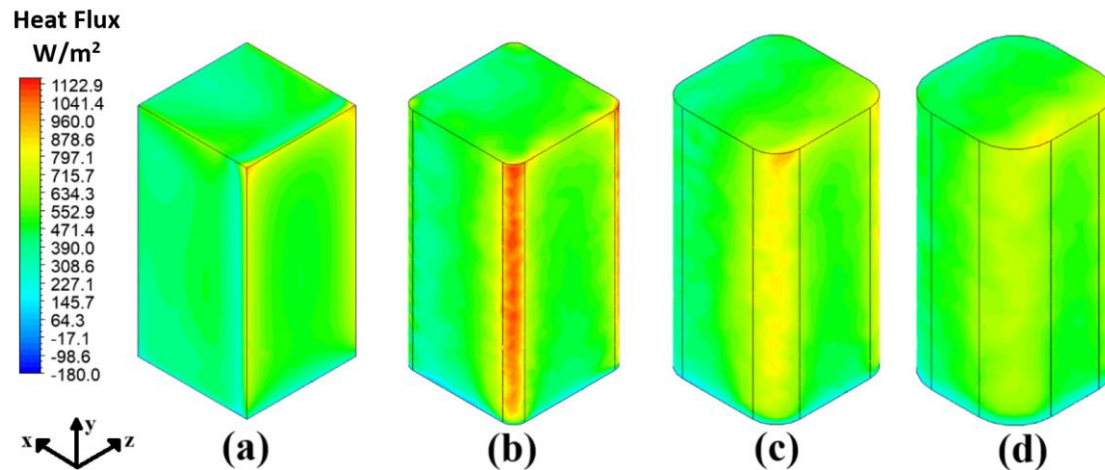


Figure 8. Heat flux in buildings with corner radius of square (a), 0.1 (b), 0.2 (c), and 0.3A (d)

IV. CONCLUSION

In this study, the effect of the corner radius on the wind flow around a prismatic building with a 1:2 aspect ratio was numerically investigated using computational fluid dynamics (CFD) methods. Four different building models were examined: one with a sharp-cornered square cross-section and three with corner radii of 0.1A, 0.2A, and 0.3A, respectively. The results obtained were evaluated comparatively.

The numerical results indicate that the corner radius has a significant influence on the flow structure around the building. In the sharp-cornered building model, early flow separation occurs at the corner regions, resulting in the formation of wide and intense wake vortices downstream of the building. In building models with applied corner radius, it was observed that the flow is directed more smoothly around the corners, flow separation is delayed, and the wake region formed behind the building is narrowed.

Pressure distribution results show that the maximum pressure values occur on the windward surfaces of all building models, while the effect of corner radius on these values remains limited. In contrast, significant changes were observed in the minimum pressure values; A transition from the square cross-section building model to the model with a 0.1A corner radius results in an approximately 68% reduction in the minimum pressure value. Increasing the corner radius to values of 0.2A and 0.3A resulted in more limited changes in the minimum pressure values.

When evaluating velocity distributions and flow lines, it was observed that the maximum velocity value was obtained in the building model with a corner radius of 0.1A, and that increasing the corner radius further resulted in a decrease in maximum velocity values. These findings demonstrate that small corner radii locally accelerate the flow, whereas larger radii lead to a more balanced flow structure.

Turbulent kinetic energy results indicate that vortex intensity and overall turbulence levels in the wake region decrease with increasing corner radius. The lowest turbulence kinetic energy values were obtained in the building model with a corner radius equal to 0.3 times the building width.

When evaluated in terms of drag coefficient, it was observed that the corner radius plays a decisive role in aerodynamic

performance. The drag coefficient calculated as 3.27 in the square-section building model decreased by approximately 28% to 2.36 in the building model with a corner radius of 0.1A. Increasing the corner radius to values of 0.2A and 0.3A resulted in more limited (2–3%) additional decreases in the drag coefficient. These results indicate that a corner radius of 0.1A represents a critical threshold value from an aerodynamic perspective.

When evaluating heat transfer results per unit volume, it was determined that switching from a square cross-section building model to a building model with a corner radius of 0.1A resulted in an approximate 31% increase in power density. Further increases in the corner radius result in only limited changes in heat transfer performance. However, increasing the corner radius to resulted in a more balanced heat flux distribution between the building facades.

In general, it has been concluded that applying corner radius to building corners provides significant advantages in terms of reducing aerodynamic drag and turbulence levels. However, it has been observed that the effect of the corner radius on the flow reaches saturation beyond a certain value, and further gains are limited. The findings highlight the importance of considering corner geometry in building aerodynamic design studies. Future studies may extend the present work by considering different wind speeds, turbulence models, and building aspect ratios.

REFERENCES

- [1] [C. O. Yigit and C. Inal, "Full-scale monitoring of wind response of a tall building using different sensors and preliminary analysis of sensor integration," *Journal of Geodesy and Geoinformation*, no. 104, pp. 30–40, 2011.
- [2] J. Liu, J. Niu, C. M. Mak, and Q. Xia, "Pedestrian level turbulent wind flow around an elevated building," *Procedia Engineering*, vol. 205, pp. 1004–1010, 2017, doi: 10.1016/j.proeng.2017.10.160.
- [3] Y. Tominaga and T. Stathopoulos, "Numerical simulation of dispersion around an isolated cubic building: Comparison of various types of $k-\epsilon$ models," *Atmospheric Environment*, vol. 43, pp. 3200–3210, 2009, doi: 10.1016/j.atmosenv.2009.03.038.
- [4] Y. Ozmen and T. Kaydok, "Numerical investigation of turbulent flow over a square cross-section high-rise building," *Kahramanmaraş Sütçü İmam University Journal of Engineering Sciences*, vol. 17, no. 2, pp. 15–25, 2015, doi: 10.17780/ksujes.38865.
- [5] J. Shao, J. Liu, and J. Zhao, "Evaluation of various non-linear $k-\epsilon$ models for predicting wind flow around an isolated high-rise building within the surface boundary layer," *Building and Environment*, vol. 57, pp. 145–155, 2012, doi: 10.1016/j.buildenv.2012.04.018.

- [6] M. Tsuchiya, S. Murakami, A. Mochida, K. Kondo, and Y. Ishida, "Development of a new k- ϵ model for flow and pressure fields around bluff body," *Journal of Wind Engineering and Industrial Aerodynamics*, vols. 67–68, pp. 169–182, 1997, doi: 10.1016/S0167-6105(97)00071-8.
- [7] S. Huang, Q. S. Li, and S. Xu, "Numerical evaluation of wind effects on a tall steel building by CFD," *Journal of Constructional Steel Research*, vol. 63, no. 5, pp. 612–627, 2007, doi: 10.1016/j.jcsr.2006.06.033.
- [8] H. Mittal, A. Sharma, and A. Gairola, "Numerical simulation of pedestrian level wind conditions: Effect of building shape and orientation," *Environmental Fluid Mechanics*, vol. 20, pp. 663–688, 2020, doi: 10.1007/s10652-019-09716-7.
- [9] T. Inan Gunaydin, "Wind flow analysis on buildings with simple plan geometries," *Megaron*, vol. 16, no. 2, pp. 286–305, 2021.
- [10] T. Inan Gunaydin, "Wind flow on and around U-shaped buildings," *Journal of Engineering, Design and Technology*, vol. 20, no. 3, pp. 841–859, 2022, doi: 10.1108/JEDT-02-2021-0104.
- [11] B. Jawhara, M. A. Alnounou, and S. Panda, "A numerical study of the effect of building height and shape on amount of wind energy available on the roof," *Materials Today: Proceedings*, vol. 74, pt. 4, pp. 1068–1073, 2023, doi: 10.1016/j.matpr.2022.12.071.
- [12] Y. Ozmen, E. Baydar, and J. P. A. J. van Beeck, "Wind flow over the low-rise building models with gabled roofs having different pitch angles," *Building and Environment*, vol. 95, pp. 63–74, 2016, doi: 10.1016/j.buildenv.2015.09.014.
- [13] Çukurova University Journal of the Faculty of Engineering and Architecture, vol. 32, no. 3, pp. 111–119, 2017.
- [14] J. C. Hu, Y. Zhou, and C. Dalton, "Effects of the corner radius on the near wake of a square prism," *Experiments in Fluids*, vol. 40, pp. 106–118, 2006, doi: 10.1007/s00348-005-0052-2.
- [15] A. Fertelli and M. Balta, "Flow analysis of two buildings arranged consecutively at different distances," *Çukurova University Journal of the Faculty of Engineering and Architecture*, vol. 35, no. 1, pp. 39–48, 2020, doi: 10.21605/cukurovaummfd.764529.
- [16] D. Golbasi, E. Buyruk, and K. Karabulut, "Experimental investigation of flow characteristics around roofless buildings arranged in triple-cross configurations at different spacings," *Muhendis ve Makina*, vol. 62, no. 704, pp. 468–485, 2021, doi: 10.46399/muhendismakina.876601.
- [17] B. Duran and H. H. Acikel, "Numerical investigation of wind loads around multiple buildings at different wind speeds," *Erciyes University Journal of Science and Technology*, vol. 38, no. 2, pp. 314–323, 2022.
- [18] T. Curebal and V. Ozmen, "Numerical investigation of the effect of the angle between two obliquely positioned buildings on velocity and pressure distributions," *Politeknik Journal*, vol. 25, no. 1, pp. 361–371, 2022.
- [19] X. Zheng, H. Montazeri, and B. Blocken, "CFD simulations of wind flow and mean surface pressure for buildings with balconies: Comparison of RANS and LES," *Building and Environment*, vol. 173, Art. no. 106747, 2020, doi: 10.1016/j.buildenv.2020.106747.
- [20] C. Nitatwichit, "Computational analysis and visualisation of wind driven naturally ventilated flows around a school building," *Maejo International Journal of Science and Technology*, vol. 2, 2008.
- [21] H. Montazeri and B. Blocken, "Numerical analysis of surface pressure coefficients for a building with balconies," in *Proc. 6th European and African Conference on Wind Engineering (EACWE)*, Cambridge, UK, 2013.
- [22] M. Ozdogan, B. Sungur, L. Namli, and A. Durmus, "Comparative study of turbulent flow around a bluff body by using two- and three-dimensional CFD," *Wind and Structures*, vol. 25, no. 6, pp. 537–549, 2017, doi: 10.12989/was.2017.25.6.537.
- [23] K. Wijesooriya, D. Mohotti, C.-K. Lee, and P. Mendis, "A technical review of computational fluid dynamics (CFD) applications on wind design of tall buildings and structures: Past, present and future," *Journal of Building Engineering*, 2023.